

Sensitivity of surface ozone over China to 2000–2050 global changes of climate and emissions



Yuxuan Wang^{a,*}, Lulu Shen^{a,c}, Shiliang Wu^b, Loretta Mickley^c, Jingwei He^{a,d}, Jiming Hao^{a,d}

^a Ministry of Education Key Laboratory for Earth System Modeling, Center for Earth System Science, Tsinghua University, Beijing, China

^b Dept. of Geological and Mining Engineering and Sciences, Dept. of Civil and Environmental Engineering, Michigan Technological University, Houghton, MI, USA

^c School of Engineering and Applied Sciences, Harvard University, Cambridge, MA, USA

^d School of Environment, Tsinghua University, Beijing 100084, China

HIGHLIGHTS

- Climate change penalty on surface ozone will be significant over East China.
- Climate change will decrease East–West ozone difference in China.
- Sensitivity of surface ozone to a given change in Chinese emissions will increase over East China but decrease over West China.

ARTICLE INFO

Article history:

Received 29 August 2012

Received in revised form

12 April 2013

Accepted 15 April 2013

Keywords:

Climate change

Ozone

China

Emissions

ABSTRACT

We use a global chemical transport model (GEOS-Chem) driven by the GISS GCM to investigate the effect on China's surface ozone from 2000 to 2050 global changes in climate and anthropogenic emissions as projected by the IPCC A1B scenario, with a focus on the different response between East and West China where present-day anthropogenic emissions, natural conditions, and ozone source attributions differ significantly. Over East China, climate change will increase both surface ozone and the possibility of high ozone episodes, implying a significant 'climate change penalty' that can be attributed mainly to increasing biogenic emissions of volatile organic compounds (VOCs). Over West China on the other hand, climate change will decrease mean surface ozone as a result of an increased ozone destruction rate in low-NO_x regimes, assuming constant stratosphere–troposphere exchange (STE) of ozone. Chinese emissions change in 2050 will enlarge the East–West ozone difference in China, but emissions change from the rest of the world (excluding China) will decrease it. Driven by climate change and emissions change in combination, nation-mean surface ozone will increase, whereas East–West ozone contrast will decrease. In the future climate, the sensitivity of surface ozone to a given change in Chinese emissions will decrease over West China due to the accelerated ozone destruction rate and reduced transport from East China, but increase over East China as a result of the coupling effect between anthropogenic NO_x and biogenic VOCs. The latter result suggests that the emission controls over East China need to be more aggressive in future climate.

© 2013 Elsevier Ltd. All rights reserved.

1. Introduction

Rapid changes of the global climate system predicted for the next 50–100 years (IPCC, 2007) will have important implications for air quality. Direct consequences of climate change for air quality may result from changes in meteorology, such as temperature,

precipitation, humidity, cloud cover, cyclone frequency, boundary layer mixing, and wet convective ventilation (Forkel and Knoche, 2006; Murazaki and Hess, 2006; Hogrefe et al., 2004; Wu et al., 2008a; Johnson et al., 1999). Natural emissions of VOCs from vegetation, NO_x from soil and lightning, the frequency of forest fires, and dust are all strongly dependent on climatic factors and are therefore sensitive to climate change. Climate change will likely enhance the stratosphere–troposphere exchange (Zeng and Pyle, 2003; Hauglustaine et al., 2005).

* Corresponding author.

E-mail address: yxw@tsinghua.edu.cn (Y. Wang).

A chemical transport model (CTM) driven by future climate archived from a general circulation model (GCM) is typically used as a computationally efficient modeling tool to capture the complex coupling between climate change and parallel changes in emissions (Jacob and Winner, 2009 and references therein). During the past decades, GCM–CTM studies on regional air quality have been mostly concerned with developed regions, focusing on the climate change penalty which tends to offset the benefit of expensive domestic emission reductions (Johnson et al., 1999; Zeng and Pyle, 2003; Wu et al., 2008a, 2008b). It is projected that economic development in developing countries is the driving factor for the overall global increase of emissions for 2000–2050 (IPCC, 2007). However, few studies have examined the consequences of parallel changes in climate and emissions on air quality in developing countries, despite the increasing importance of rising emissions from them on global atmospheric environment.

We present here a numerical study aiming to understand the extent and mechanism of surface ozone changes in China in response to a particular scenario of 2000–2050 global changes, using a global CTM (GEOS-Chem) driven by the GISS GCM. It is not a quantitative prediction of future ozone levels in China. The difference in ozone origins between East and West China in present-day condition (Wang et al., 2011) will imply different responses of surface ozone to future changes in climate and anthropogenic emissions, which will be the focus of this study. Through an ensemble of model sensitivity analysis, we evaluate the separate and combined effects on surface ozone from the projected changes in climate, Chinese anthropogenic emissions (CHE), and anthropogenic emissions from the rest of the world (RWE). The implication of our analysis for air quality policies in China will be discussed.

2. Model and simulations

2.1. Description of the model and emissions

We use the NASA/GISS GCM 3 (Rind et al., 2007) to simulate the present-day and 2050 climate based on the IPCC A1B emission scenario of greenhouse gases. The GISS model version used here has a horizontal resolution of 4° (latitude) \times 5° (longitude) and 23 sigma levels up to 0.002 hPa. Meteorological output from the GISS model was archived to drive the GEOS-Chem global chemical transport model which runs with the same spatial resolution as the GISS GCM (Wu et al., 2007). The model set up is the same as in Wu et al. (2008a) and we do not give detailed description here.

The GEIA (Global Emission Inventory Activity) inventory (Benkovitz et al., 1996) is the baseline anthropogenic inventory in GEOS-Chem and is overwritten by regional emission inventories when available. The present-day anthropogenic emission inventories adopt 2000 as the base year. Scale factors based on energy statistics and other information are used to obtain the emission inventory for the base year, as implemented by van Donkelaar et al. (2008) following on the work of Bey et al. (2001) and Park et al. (2004). Anthropogenic emissions from East Asia are taken from the inventory of Zhang et al. (2009) that is publicly available and has been extensively used by chemical transport models. Biogenic emissions of nonmethane VOCs (NMVOCs) are calculated online in GEOS-Chem with the Model of Emissions of Gases and Aerosols from Nature (MEGAN) scheme (Guenther et al., 2006). The present-day emissions of isoprene over China from the MEGAN inventory are 50% smaller than those from the GEIA biogenic emission inventory used by Wu et al. (2008a). Biomass burning emissions are taken from the GFED-2 inventory (van der Werf et al., 2006). The future changes in global anthropogenic emissions of ozone precursors are based on the IPCC A1B emission scenario. Wu et al. (2008a) presented the regional-specific scaling factors derived

from the A1B scenario to obtain 2050 emissions on the basis of 2000 emissions. The same scaling factors are used in this study, resulting in the same 2000–2050 emission trends by world regions as in Wu et al. (2008a) but slightly different global total emissions because of the differences in the present-day emission inventories discussed above. The same species-specific scaling factors as in Wu et al. (2008a) are used to obtain the biomass burning emissions in 2050 on the basis of 2000 emissions. The possible coupling effect of climate change on biomass burning (Jeong and Wang, 2010) is not considered in this study. The methane mixing ratios used for the present-day scenario is specified with a global mean of 1750 ppb and 5% inter-hemispheric gradient, rising to 2400 ppb by 2050 with no hemispheric gradient in the future scenario. The emission inventory used in this study is summarized in Table 1.

We do not account for the possible change in stratosphere–troposphere exchange (STE) of ozone in the future climate, which is kept constant with a global total STE ozone flux of 500 Tg yr^{-1} . Though an STE change has potential importance for surface ozone over Tibetan Plateau, we choose to keep STE constant from 2000 to 2050 in this study in order to focus our attention on the impact from tropospheric climate change and anthropogenic emission change.

2.2. Model simulations and evaluation

We separate the contributions from climate and emission changes through a sensitivity analysis. To cover the full array of combinations for 2000–2050 changes in climate, CHE, and RWE, eight numerical cases are set up and summarized in Table 2. To account for the interannual variability, each simulation is conducted for three years, 1999–2001 for the present-day climate and 2049–2051 for the future climate. The case pairs that differ by a single factor are compared to analyze the effect of that factor on ozone. For example, the difference between case B and A (denoted as B–A) indicates the CHE-only effect on surface ozone under the present-day climate. Unless noted otherwise, all the results shown in this paper refer to annual-mean afternoon (noon to 5 pm local time) mixing ratios of ozone at the surface.

Quantitative comparisons between numerical simulations shown in this study are based primarily on the national-mean ozone over China. At the sub-country scale, China features pronounced East–West contrasts in important natural (e.g., topography, climate, land type) and social–economic factors (e.g., population, GDP, anthropogenic emissions) that are expected to have significant influence on the spatial distribution of ozone. East China is a region of large population and intensive agriculture, accounting for 68% of China's population, 76% of its GDP, and 62% of its anthropogenic NO_x emissions in the present day, as showed in Fig. 1. As the East–West contrast is on a spatial scale larger than 1000 km, it can be captured by our model (c.f. Fig. 1c). West and East China are defined as the regions shown in Fig. 1c. Table 2 gives the annual- and summer-mean surface ozone averaged over China, the associated spatial deviations (in parenthesis), and the annual mean East–West ozone difference simulated by the model for each sensitivity case.

Due to the nonlinear ozone response to precursor concentration levels, excessive spatial averaging of emissions by coarse resolution of the model ($4^\circ \times 5^\circ$) will lead to systematic overestimation of regional O_3 production (Sillman et al., 1990). Wild and Prather (2006) investigated the impact on ozone production over East Asia of different model resolutions. They found a 7% reduction in net regional production as model resolutions increasing from $5.6^\circ \times 5.6^\circ$ to $1.1^\circ \times 1.1^\circ$. The potential bias in overestimating ozone production as a result of the coarse model resolution is expected to cancel out to some extent in this study as we focus on the ozone

Table 1
The 2000–2050 trends in anthropogenic and natural emissions of ozone precursors.

		World			China		
		2000	2050	Change (%)	2000	2050	Change (%)
NO _x (Tg a ⁻¹)	Aircraft	0.51	0.51	0.0	0.02	0.02	0.0
	Fossil fuel	24.2	43.3	78.6	2.69	5.19	93.0
	Biomass burning	5.25	6.36	21.1	0.037	0.009	-76.5
	Biofuel	2.21	2.10	-4.6	0.49	0.32	-35.5
	Fertilizer	0.47	0.91	96.5	0.069	0.053	-23.2
	Lightning	4.92	5.79	17.6	0.25	0.32	25.8
	Soil	6.73	7.69	14.3	0.32	0.33	3.7
CO (Tg a ⁻¹)	Biomass burning	381.5	610.3	60.0	3.04	0.84	-72.4
	Biofuel	175.2	168.3	-3.9	43.3	27.8	-35.8
	Anthropogenic	331.0	397.7	20.2	94.9	84.7	-10.7
	Monoterpenes	48.52	69.0	42.1	1.3	1.3	0
VOCs (Tg C a ⁻¹)	Anthropogenic	48.7	127.8	160.2	7.02	12.8	81.6
	Biomass burning	12.5	21.4	70.7	0.25	0.077	69.2
	Methane (ppb)	1750	2400	37.1	N/A		
BC (10 ⁶ kg)	Anthropogenic	3.45	2.24	-35.1	0.94	0.29	-69.6
	Biomass burning	2.57	2.62	1.9	0.017	0.016	-6.5
	Biofuel	1.63	0.62	-61.8	0.40	0.17	-57.4
OC (10 ⁶ kg)	Anthropogenic	2.69	1.03	-61.9	0.65	0.17	-73.3
	Biomass burning	20.2	20.6	2.0	0.22	0.18	-16.1
	Biofuel	7.05	2.95	-58.1	1.44	0.64	-55.5
	Biogenic	106.2	145.8	37.2	2.82	3.89	38.3
Isoprene (Tg C a ⁻¹)		347.5	492.5	41.7	5.18	6.94	34.1
Other biogenic NMVOCs (Tg C a ⁻¹)		155.3	213.0	37.1	3.54	4.69	32.4
Anthropogenic SO ₂ (Tg S)		50.1	75.2	50.1	9.8	7.8	-20.4
Anthropogenic NH ₃ (Tg)		45.2	61.7	36.5	15.0	13.1	-12.7

changes between model sensitivity simulations. As the present GISS-driven GEOS-Chem model has only a 4ox5o-resolution version, we compare in Fig. 2 the summer-mean GEOS-Chem model results driven by the NASA GEOS-5 assimilated meteorology at two resolutions: 0.5° × 0.667° (2a) and 4° × 5° (2c). For easier comparison, Fig. 2b shows the same 0.5° × 0.667° model results averaged onto the 4ox5o grids. The 4° × 5° model shows the same large-scale feature of ozone distribution over China as the finer-resolution model. The national-mean surface ozone mixing ratio simulated by the coarse resolution model (4° × 5°) differ by about 2% (1 ppbv) compared with that simulated by the finer-resolution model (0.5° × 0.667°). Based on the comparison, we argue that the current resolution of the model (4° × 5°) is sufficient as far as ozone changes at the national and sub-national scale (i.e., East China and West China mean) are concerned.

As this study examines the large-scale spatial pattern of annual-mean surface ozone changes across China, satellite data are more suitable for the purpose of model evaluation than sparsely distributed surface observations in China from the literature. Here we adopt tropospheric ozone products from Tropospheric Emission Spectrometer (TES) aboard the NASA Aura satellite, which is capable of retrieving ozone concentrations in the lower

troposphere with 1–3 pieces of information (Beer, 2006; Nassar et al., 2008). TES version 4 level-3 ozone mixing ratios at 825 hPa averaged over a period of five years (2005–2009) (<http://tes.jpl.nasa.gov/>) are used to evaluate the corresponding model output of the present-day case (case A) in Fig. 3. The averaging kernels associated with the TES ozone retrieval are applied to the model profiles to derive the simulated ozone mixing ratios at 825 hPa (Fig. 3a) for comparison with TES retrieval. The TES retrieval products at 825 hPa are scarce over the high-elevated Tibet Plateau region (shown in white in Fig. 3b), and we exclude this part of data in the validation. Consistent with the spatial pattern from TES, the model successfully reproduces the high ozone regions over North China and India as well as the concentration gradient within the continent and from continent to ocean. Fig. 3c presents the scatter plot of monthly-mean ozone mixing ratio at 825 hPa between model (with TES averaging kernels applied) and TES over East Asia. The square of the correlation coefficient between model and TES is 0.92, lending confidence to the model's ability of simulating the large-scale spatial and temporal heterogeneity of ozone within East Asia. The model has a bias of -6 ppbv on average compared to TES, which can be partly explained by the different time range between model (1999–2001) and TES (2005–2009).

Table 2
The afternoon-mean surface ozone and East–West ozone difference over China under 8 different scenarios.

Case label	Description	Afternoon-mean surface ozone over China		East–West ozone difference
		Annual mean (std deviation)	Summer mean (std deviation)	Annual-mean
A	2000 climate + 2000 RWE + 2000 CHE	45.7 ± 10.2	47.0 ± 10.7	3.4
B	2000 climate + 2000 RWE + 2050 CHE	47.9 ± 12.0	51.7 ± 12.7	4.9
C	2000 climate + 2050 RWE + 2000 CHE	52.1 ± 12.9	53.7 ± 12.8	-1.9
D	2000 climate + 2050 RWE + 2050 CHE	54.5 ± 14.4	58.6 ± 14.3	0.71
E	2050 climate + 2000 RWE + 2000 CHE	45.7 ± 10.8	47.4 ± 11.9	4.3
F	2050 climate + 2000 RWE + 2050 CHE	47.9 ± 12.8	52.2 ± 14.3	6.3
G	2050 climate + 2050 RWE + 2000 CHE	52.0 ± 13.2	54.0 ± 13.4	-1.0
H	2050 climate + 2050 RWE + 2050 CHE	54.4 ± 14.9	58.9 ± 15.4	2.1

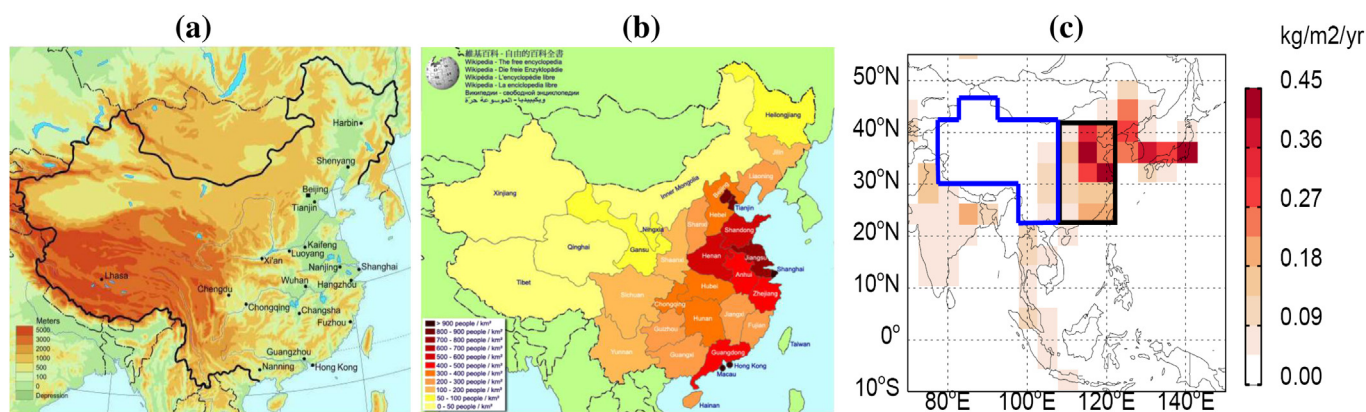


Fig. 1. (a) Topography (meters) of China; (b) China's population density by provinces (http://en.wikipedia.org/wiki/List_of_People%27s_Republic_of_China_administrative_divisions_by_population_density; accessed Feb 6, 2012); (c) present-day anthropogenic NO_x emissions over China. The black and blue regions shown in 1c indicate East China and West China respectively as defined in this study. (For interpretation of the references to color in this figure legend, the reader is referred to the web version of this article.)

3. Effect of climate change alone

The 2000–2050 changes in summertime temperature, precipitation, and PBL (planetary boundary layer in 1200–1600 local time) height simulated by the GISS GCM are presented in Fig. 4a–c respectively. We calculate that the 2000–2050 climate change will result in a 34% increase in isoprene emissions in China as a result of higher temperature and solar radiation (Guenther et al., 2006; Wang et al., 1998). There is a maximal decrease of 20% in PBL height over East China, but decreases over other regions in China. Although there appears to be an association between PBL decrease and ozone increase over East China, we cannot establish a causal relationship because of the compounding effects of other factors and the large uncertainty in predicting PBL height (Jacob and Winner, 2009). Although predicted precipitation in future climate tends to differ among different models, we found that the precipitation distribution over China predicted by the GISS model agrees well with the mean model results summarized by IPCC (Supplementary material, S.1). The GISS-predicted future changes of wind speed, humidity, column cloud fraction and solar radiation and their relationship with ozone are also presented in more detail in the Supplementary material, S.2.

The annual-mean ozone difference between Case E and Case A (Fig. 5b), representing the climate-only effect on surface ozone under the present-day anthropogenic emissions, is negative over

West China and positive over East China. When averaged over the whole country, the difference is small (-0.1 ± 3.1 ppbv) because of the offsetting effect between East and West China. The climate-driven ozone increase over East China is most pronounced and spatially extensive in summer, reaching to a maximum of 10 ppbv in some areas. The East–West ozone difference is 3.4 ppbv in present day (Case A), which increases by 0.9 ppbv (27%) in the 2050 climate case (Case E) and this change is statistically significant with $p < 0.05$.

The cumulative probability distributions of monthly-mean surface ozone for selective cases (A, E, and H) are showed in Fig. 6a. The significant difference at the high end suggests that the possibility of high ozone episodes will increase in future climate, especially over East China. Fig. 6b displays the cumulative probability distribution of monthly-mean ozone differences driven by climate-change alone under the present-day (Case E–A; black curve) and 2050 emissions (Case H–D; red curve). Climate change leads to both positive and negative changes on surface ozone regardless of emission levels. Surface ozone over West China decreases in the 2050 climate with the largest reduction of -5 ppbv, indicating a ‘climate change benefit’. In contrast, ozone increases over East China by a maximum of 10 ppbv on the monthly-mean basis which implies a significant ‘climate change penalty’ over the densely-populated East China. The annual climate penalty is 0.55 ± 3.8 ppbv over East China and climate benefit

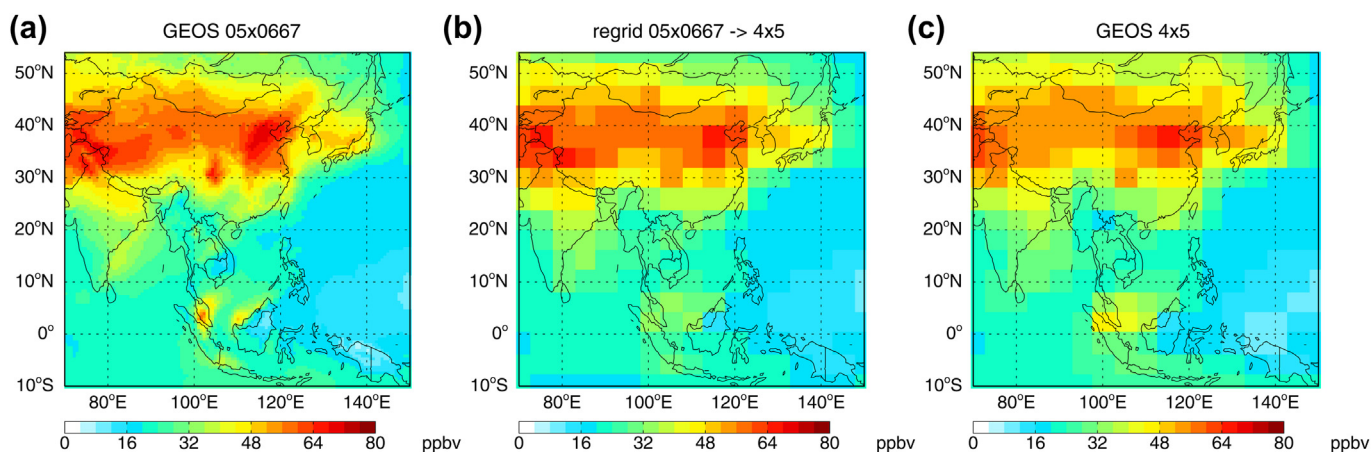


Fig. 2. 2006 summer-mean ozone spatial distribution between GEOS-5 0.5x0.667 and 4x5 resolution. (a) ozone distribution under 0.5x0.667 resolution; (b) regrid the 0.5x0.667 results to 4x5 resolution; (c) ozone distribution under 4x5 resolution.

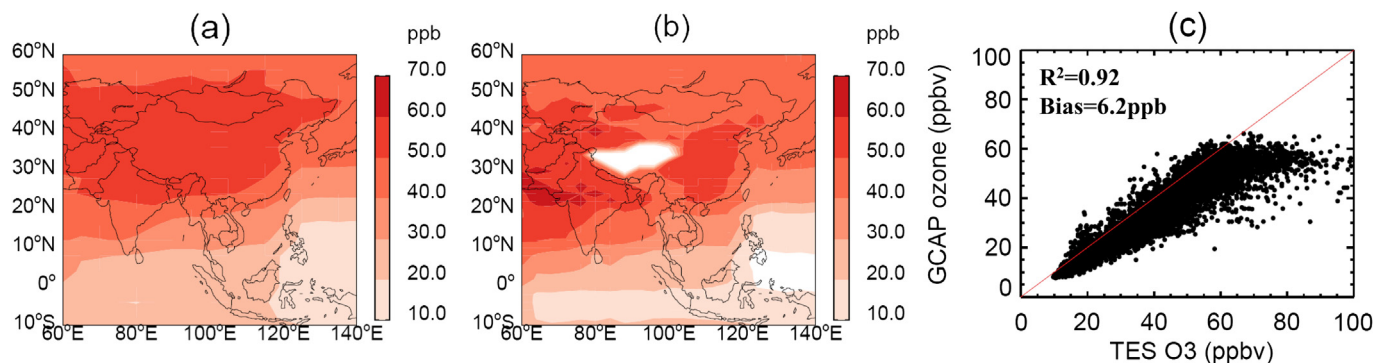
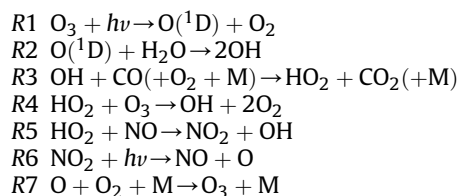


Fig. 3. (a) Ozone distribution at 825 hPa simulated by the model (with TES averaging kernels applied) for the present-day case (case A); (b) Ozone distribution at 825 hPa retrieved by TES minus 6.2 ppbv throughout the domain. The -6.2 ppbv refers to the mean difference between TES and model determined in (c); (c) Scatter plot between model (y-axis) and TES ozone (x-axis). The red line is the $y = x$ line. (For interpretation of the references to color in this figure legend, the reader is referred to the web version of this article.)

is -0.37 ± 2.7 ppbv over West China (both statistically significant with $p < 0.05$). As a result, climate change has significantly changed the mean distribution of surface ozone in China, increasing the East–West ozone difference under the present-day and 2050 emissions.

The following reactions (R1–R7) present the main reactions of O_3 formation and destruction in the troposphere (Seinfeld and Pandis, 1998).



The increase of water vapor in the 2050 climate accelerates the destruction of ozone through R2, which results in decreased ozone lifetime and therefore lower surface ozone over remote regions, particularly over the oceans. Climate change reduces PAN stability due to higher temperature, leading to reduced ozone background over continental regions (Johnson et al., 1999; Murazaki and Hess, 2006). Climate change also leads to increasing HO_2 , which plays an important role in destroying O_3 in low- NO_x regions through R4 (Lelieveld et al., 2002, 2004). Wang et al. (2011) suggested that the dominant component of surface ozone over West China where anthropogenic emissions are small is hemispheric background. Therefore, the decrease of surface ozone over West China can be attributed to reduced ozone background in low- NO_x regions as a result of accelerated ozone destruction rate and reduced PAN

stability as a proxy of long-range transport of NO_x in the future climate.

Over regions where NO_x is in abundant supply, increases in HO_2 will lead to enhanced ozone production through R5–R7. Under the present-day emissions, the climate change penalty over East China has a summer-average of 1.7 ± 3.6 ppbv. It can reach up to 10 ppbv in some areas (Fig. 6b), posing significant implications for public health given the large population in East China (874 million in 2005). In this region, the climate change penalty arises from the combination of enhanced natural emissions of ozone precursors (c.f. Table 1) and changes in meteorological factors including higher temperature and higher water vapor content as discussed above. We conduct a sensitivity simulation in which biogenic emissions of VOCs over China in the 2050 climate are scaled down to their emission levels in 2000 in order to remove the role of increasing biogenic VOCs on ozone in the 2050 climate. In this case, the annual climate change penalty over East China is reduced by 40% (Fig. 5c). This implies that over 40% of the climate change penalty could be attributed to increases in biogenic emissions of VOCs, with the balance resulting from changes in meteorology, including higher temperatures, lower PBL heights, and reduced ventilation rates.

4. Effect of emission changes alone

As shown in Table 2, the 2000–2050 change in CHE alone will increase surface ozone by 2.2 ± 3.3 ppbv over China under the present-day climate and RWE (Case B–A). The ozone increase is pronounced in East China (3.35 ± 4.77 ppbv) but much smaller in West China (1.84 ± 1.72 ppbv). The CHE-only effect on annual-mean surface ozone distribution is illustrated in Fig. 7a. The largest

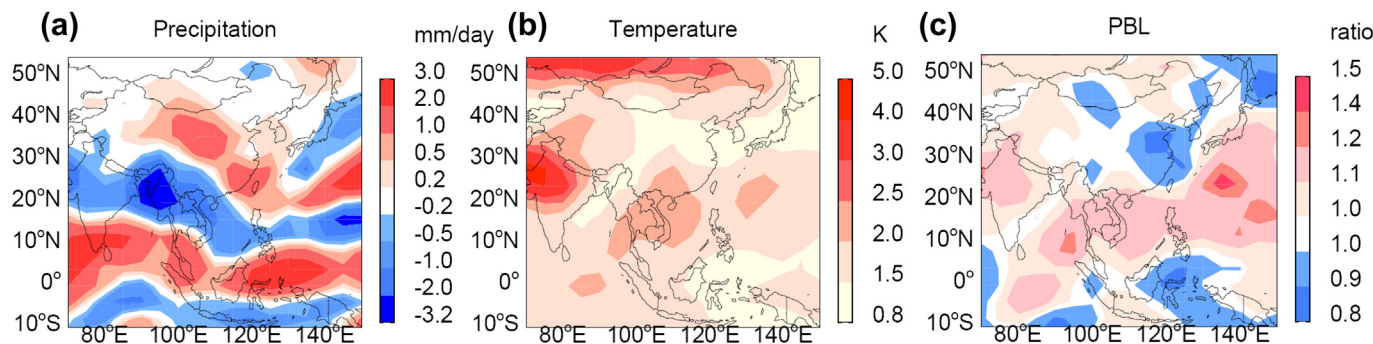


Fig. 4. The 2000–2050 change in summertime (a) precipitation, (b) temperature, (c) planetary boundary layer depth (PBL) as simulated by the GISS model.

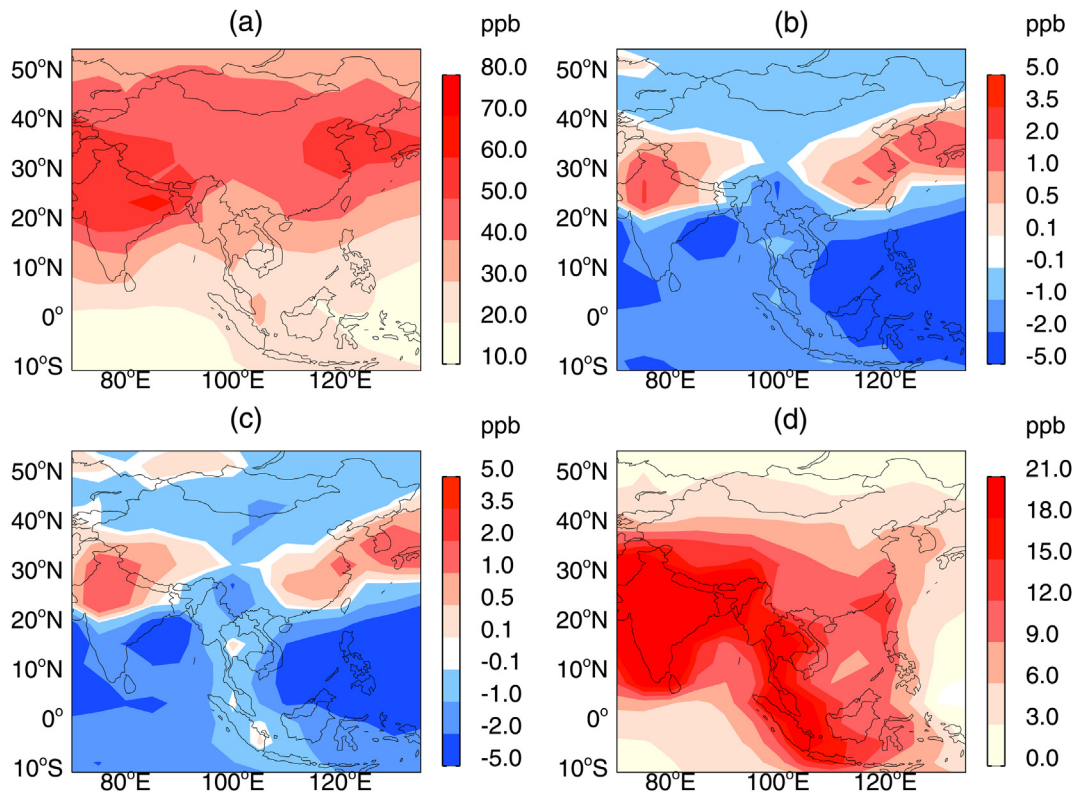


Fig. 5. (a) The annual-mean distribution of surface ozone over China in the present-day climate and emissions (Case A); (b) The climate-only effect on annual-mean surface ozone (Case E-A); (c) same as b, but without the increase in biogenic emissions of VOCs in the 2050 climate; (d) the combined effect of the 2000–2050 global changes in both climate and emissions on annual-mean distribution of surface ozone over China (Case H-A).

increase is in the southeast, reaching 5–10 ppbv. Over the southern regions (south of 30°N), the 2000–2050 change in CHE will result in increasing surface ozone in all seasons. In contrast, no significant increase is found north of 35°N in winter and spring because lower temperature and weak solar radiation over this region are the limiting factors for ozone formation instead of precursor emissions. Similar to climate change that decreases the East–West ozone difference, the CHE change alone results in an increase in the East–West ozone difference by 1.5 ppbv–4.9 ppbv under 2050 CHE and the change is significant.

The 2000–2050 change in RWE alone (Case C–A) will increase surface ozone by 6.4 ± 4.7 ppbv over China under the present-day climate and CHE. The distribution of annual-mean surface ozone change is illustrated in Fig. 7b. The effect of RWE change alone shows a decreasing gradient from west to east and from south to north, reflecting different emission trends in surrounding countries/regions. The effect of RWE change alone is to decrease the East–West ozone difference by about 5.3 ppbv to –1.9 ppbv (2050 RWE). The largest surface ozone increase is in southwest China and the Tibet Plateau, reaching 6 ppbv. This can be largely attributed to

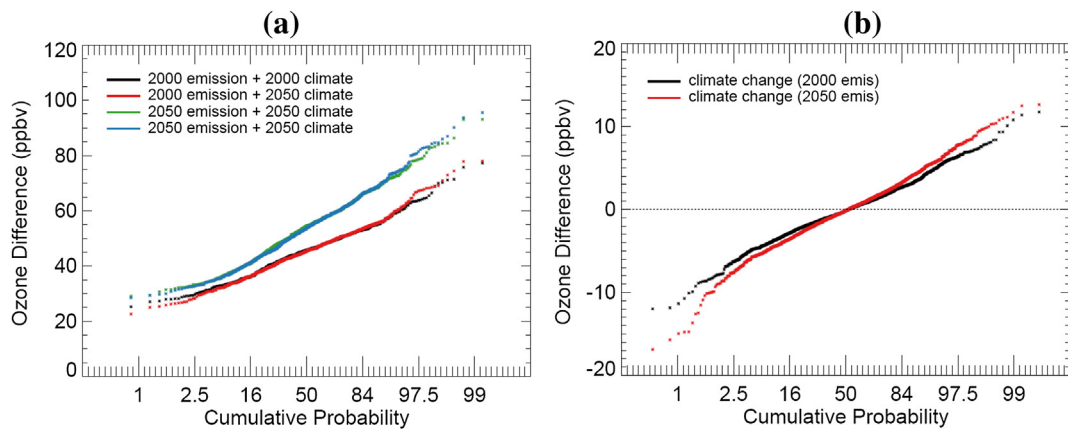


Fig. 6. (a) The ozone cumulative probability distribution under different scenarios over China. Each point represents the mean surface ozone mixing ratio at each grid-box in every month of the year. (b) The cumulative probability of surface ozone differences driven by climate change only under 2000 emissions (black) and 2050 emissions (red) over China. The black line in (b) represents the cumulative probability distribution of the difference between the blue and black curves shown in (a), and the red line in (b) represents the difference between the red and blue curves in (a). (For interpretation of the references to colour in this figure legend, the reader is referred to the web version of this article.)

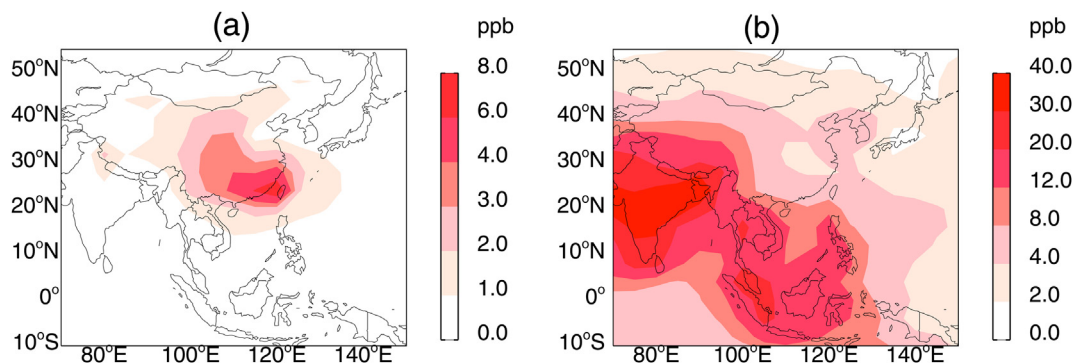


Fig. 7. The effect of the 2000–2050 emission changes on annual-mean surface ozone over China under the present-day climate: (a) Chinese emission changes only (CHE change only), (b) Rest of world emission changes only (RWE change only).

increasing anthropogenic emissions from India. The A1B scenario forecasts that Indian anthropogenic emissions of NO_x and VOCs will increase by 800% and 300% respectively from 2000 to 2050. The challenge for policy-makers to protect the fragile ecosystems over the Tibetan Plateau and Himalayan Glaciers is to find an effective trans-boundary pollution control policy involving both China and India.

5. Effect of climate change on ozone sensitivity to domestic emissions

The question of interest in this section is whether a given change in emissions (domestic or foreign) will result in the same magnitude of ozone change in the future climate as compared with the present-day climate. We focus on the difference in the emission-only effect between the present-day and future climate. For example, Case B–A gives the CHE-only effect under the present-day climate, while Case F–E yields the CHE-only effect under the 2050 climate. The difference between the two CHE-only effects represents the climate-driven change in the sensitivity of ozone to domestic emissions.

The spatial distribution of the difference in the CHE-only effect between 2000 and 2050 climate is presented in Fig. 8a for the summer-mean condition. The CHE-driven change in the East–West annual-ozone difference is 0.47 ppbv larger under the 2050 climate than that under the present-day climate. Although

these differences appear small in magnitude, they are statistically significant given the large spatial variability of the CHE-only effect over the whole country. Fig. 9a presents the cumulative probability distribution of the summer-mean CHE-only effect on surface ozone under the present-day climate (black line) and 2050 climate (red line). Although the black and red curves are similar in shape, their differences are significant both in the high and low end of the distribution. Fig. 9b presents the cumulative probability distribution of the summertime difference in the CHE-only effect between 2000 and 2050 climate (paired by grid box and month) for China as a whole (blue), East China (orange), and West China (purple). Taking China as a whole, the negative points on the blue line are mainly located in the relatively clean West China region and the positive points located in East China (c.f. Fig. 8a). The contrast between East and West China is very clear: all the grid boxes over East China show increases in the sensitivity to domestic emissions in the future climate whereas over 90% of the grid boxes over West China show decreases. Hypothesis testing shows that the difference is significant with $p < 0.05$.

The results suggest that a given increase in CHE will result in a larger increase in surface ozone under the 2050 climate when biogenic VOCs emissions are higher and background ozone is lower (Wu et al., 2008a). The policy implication is that a slower rate of increase in domestic emissions will be required to meet a given ozone air quality target in the 2050 climate over those

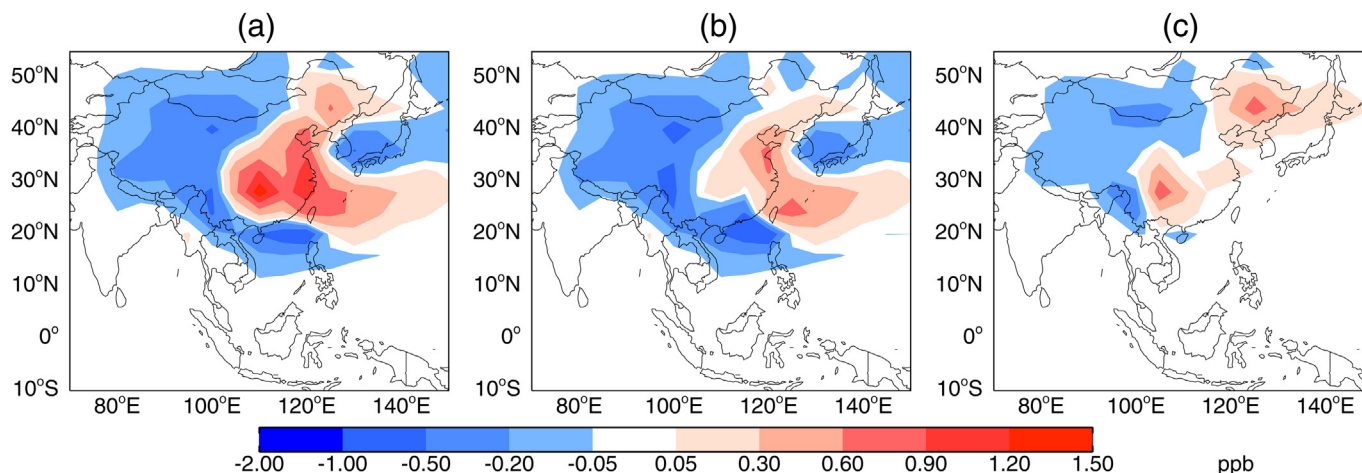


Fig. 8. (a) The summer-mean difference in the effect of the 2000–2050 Chinese emission change on surface ozone between the 2000 and 2050 climate; (b) same as a, but without the changes in biogenic emissions of VOCs as a function of climate change; (c) same as a, but without the changes in the anthropogenic emissions over East China.

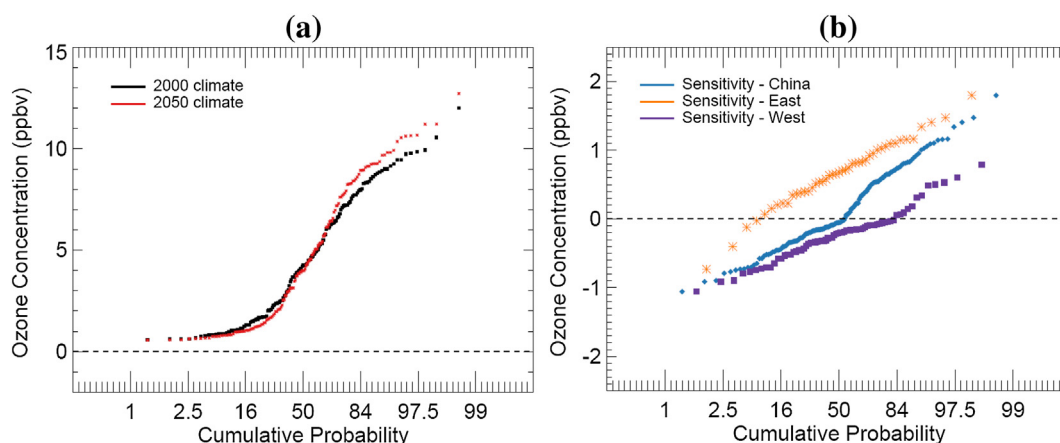


Fig. 9. (a) Cumulative probability distribution of the summer-mean effect of the 2000–2050 Chinese emission changes on surface ozone under the 2000 climate (black line; Case B–A) and 2050 climate (red line; Case F–E). Each point represents mean surface ozone mixing ratio at each grid-box in each month in summer. (b) The cumulative probability distribution of the differences between the black and red curves in (a) by region (Case (F–E)–(B–A)): blue curve for all the grid boxes in China, orange for East China, and purple for West China. (For interpretation of the references to colour in this figure legend, the reader is referred to the web version of this article.)

Table 3

The effect of the 2000–2050 global changes on annual afternoon-mean surface ozone over East China, West China, and the East–West ozone differences.

Factors	East China		West China		East–West
	ppbv (standard deviation)	Percentage	ppbv (standard deviation)	Percentage	ppbv (standard deviation)
2000–2050 change in Chinese emissions ^a	4.1 ± 5.0	45%	1.8 ± 1.7	17%	2.3
2000–2050 change in world emissions (excluding China) ^b	4.2 ± 1.7	47%	9.0 ± 4.7	87%	–4.8
2000–2050 change in climate	0.7 ± 4.2	8%	–0.5 ± 3.0	–4%	1.2
Combined changes ^c	9.0	100%	10.3	100%	–1.3

^a Referred to as CHE in the text.

^b Referred to as the rest of the world emissions (RWE) in the text.

^c Here we mean the combination of the 2000–2050 changes in the three factors (CHE, RWE, and climate).

regions where the sensitivity of ozone to domestic emissions will increase as a result of climate change. When we do not allow biogenic emissions (all over the world) to change in the 2050 climate, the increase of ozone sensitivity to CHE almost diminishes over East China while the decrease of sensitivity over West China still persists (Fig. 8b). This suggests that the coupling between increasing biogenic VOCs and anthropogenic NO_x emissions as suggested by Wu et al. (2008a) is not the mechanism responsible for the decrease of ozone sensitivity to CHE over West China. We conduct a sensitivity simulation in which anthropogenic emissions over East China do not change in 2050. The corresponding change in ozone sensitivity for this case, shown in Fig. 8c, is 30% less than that in Fig. 8a over West China. This suggests that surface ozone over West China in the 2050 climate is less sensitive not only to anthropogenic emissions locally but also to those over East China, with the former contributing 70% of the overall change in sensitivity and the latter 30%.

6. Combined effect of global change on surface ozone

The differences between Case A (2000 climate and emissions) and Case H (2050 climate and emissions) represent the response of surface ozone to the combined effect of 2000–2050 changes in climate and anthropogenic emissions of ozone precursors. Fig. 5d shows the simulated changes in surface ozone over China in 2050 relative to the present-day case (Fig. 5a). Annual mean surface ozone will increase by 8.7 ppb over China (Fig. 5d), compared with the mean global change of 4.6 ppbv (not shown). Over East China the increase in surface ozone will reach an average of

16 ppbv in the summer. The large increase of surface ozone over East China will have important implications for public health and ecosystem.

Table 3 summarizes the mean CHE-only, RWE-only, climate-only, and the combined effects over East China, West China, and the East–West ozone difference. CHE and climate change will enhance the East–West ozone difference while RWE will decrease it. For the heavily populated East China region, the contributions from the change in CHE and RWE are comparable, responsible for 45% and 47% of the total effect respectively. Most importantly, climate change represents a large positive effect (8%) over this region, resulting in a significant climate-change penalty. As we suggest above, an aggressive emission control strategy is required to cope with this trend.

The impact from climate change alone is smaller as compared with emission changes alone. But climate change and emission change will occur in parallel in the future and the interaction between them cannot be neglected. As indicated in the sensitivity analysis, climate change will increase the sensitivity of surface ozone to a given change in domestic emissions by 8% over East China. Given the large population in East China, this climate-change penalty needs to be considered, calling for more stringent emission control policies in future climate compared with those available today.

7. Conclusion and discussion

We investigated the effects of 2000–2050 global changes on surface ozone over China using the GEOS-Chem model with

meteorological inputs provided by the GISS GCM. The projection of global anthropogenic emissions of ozone precursors are based on the IPCC A1B scenario. We decompose future global changes into three factors: climate, CHE and RWE. We find that climate change leads to an increase of ozone in East China but a decrease in West China and that 40% of the climate change penalty over East China could be attributed to the increase in biogenic emissions of VOCs. Climate change enlarges the East–West ozone difference by 0.9 ppbv and 1.4 ppbv respectively under the present-day and 2050 emissions (both with $p < 0.05$).

The changes in CHE alone result in an increase of 2.2 ppbv in surface ozone over China and an increase of the East–West ozone difference by 1.5 ppbv. The changes in RWE alone result in an increase of 6.4 ppbv in surface ozone for China, but decreases the East–West ozone difference by about 5.3 ppbv. In the A1B emission scenario, surface ozone levels over southwest China and the Tibet Plateau will increase by 10–15 ppbv in the summer. The 2000–2050 climate change will increase the sensitivity of summer surface ozone to domestic anthropogenic emissions by about 8% over East China, but decrease this sensitivity over West China. The increased sensitivity to CHE in the 2050 climate implies that domestic emission controls over China need to be more aggressive in the future.

Acknowledgments

This research was supported by the National Science Foundation of China (grant No. 41005060) and by the Beijing Nova Program (Z121109002512052). S. Wu acknowledges support from the US EPA STAR Grant R83428601, and L. Mickley acknowledges support from the US EPA STAR Grant RD-83337001. EPA has not officially reviewed or endorsed this publication, and the views expressed herein may not reflect those of EPA. TES data is managed by NASA Jet Propulsion Laboratory (JPL) and we thank Dr. M. Luo at JPL for providing the TES ozone data.

Appendix A. Supplementary data

Supplementary data related to this article can be found at <http://dx.doi.org/10.1016/j.atmosenv.2013.04.045>.

References

- Beer, R., 2006. TES on the Aura mission: scientific objectives, measurements, and analysis overview. *IEEE Transactions On Geoscience And Remote Sensing* 44 (5), 1102–1105.
- Benkovitz, C.M., Scholtz, M.T., Pacyna, J., Tarrason, L., Dignon, J., Voldner, E.C., Spiro, P.A., Logan, J.A., Graedel, T.E., 1996. Global gridded inventories of anthropogenic emissions of sulfur and nitrogen. *Journal of Geophysical Research* 101 (D22), 29,239–29,253.
- Bey, I., Jacob, D.J., Yantosca, R.M., Logan, J.A., Field, B.D., Fiore, A.M., Li, Q., Liu, H.Y., Mickley, L.J., Schultz, M.G., 2001. Global modeling of tropospheric chemistry with assimilated meteorology: model description and evaluation. *Journal of Geophysical Research* 106 (D19), 23,073–23,095. <http://dx.doi.org/10.1029/2001JD000807>.
- Forkel, R., Knoche, R., 2006. Regional climate change and its impact on photo-oxidant concentrations in southern Germany: simulations with a coupled regional climate-chemistry model. *Journal of Geophysical Research* 111, D12302. <http://dx.doi.org/10.1029/2005JD006748>.
- Guenther, A., Karl, T., Harley, P., Wiedinmyer, C., Palmer, P.L., Geron, C., 2006. Estimates of global terrestrial isoprene emissions using MEGAN (Model of Emissions of Gases and Aerosols from Nature). *Atmospheric Chemistry and Physics* 6, 3181–3210. <http://dx.doi.org/10.5194/acp-6-3181-2006>.
- Hauglustaine, D.A., Lathière, J., Szopa, S., Folberth, G.A., 2005. Future tropospheric ozone simulated with a climate-chemistry-biosphere model. *Geophysical Research Letters* 32, L24807. <http://dx.doi.org/10.1029/2005GL024031>.
- Hogrefe, C., Lynn, B., Civerolo, K., Ku, J.Y., Rosenthal, J., Rosenzweig, C., Goldberg, R., Gaffin, S., Knowlton, K., Kinney, P.L., 2004. Simulating changes in regional air pollution over the eastern United States due to changes in global and regional climate and emissions. *Journal of Geophysical Research* 109, D22301. <http://dx.doi.org/10.1029/2004JD004690>.
- IPCC (Intergovernmental Panel on Climate Change), 2007. Climate change. In: Solomon, S., et al. (Eds.), *The Scientific Basis. Contribution of Working Group I to the Fourth Assessment Report of the Intergovernmental Panel on Climate Change*. Cambridge Univ. Press, New York.
- Jacob, D.J., Winner, D.A., 2009. Effect of climate change on air quality. *Atmospheric Environment* 43, 51–63. <http://dx.doi.org/10.1016/j.atmosenv.2008.09.051>.
- Jeong, G.R., Wang, C., 2010. Climate effects of seasonally varying biomass burning emitted carbonaceous aerosols (BBCA). *Atmospheric Chemistry and Physics* 10, 8373–8389. <http://dx.doi.org/10.5194/acp-10-8373-2010>.
- Johnson, C.E., Collins, W.J., Stevenson, D.S., Derwent, R.G., 1999. Relative roles of climate and emissions changes on future tropospheric oxidant concentrations. *Journal of Geophysical Research* 104 (D15), 18,631–18,645. <http://dx.doi.org/10.1029/1999JD900204>.
- Lelieveld, J., Peters, W., Dentener, F.J., Krol, M.C., 2002. Stability of tropospheric hydroxyl chemistry. *Journal of Geophysical Research* 107 (D23), 4715. <http://dx.doi.org/10.1029/2002JD002272>.
- Lelieveld, J., Dentener, F.J., Peters, W., Krol, M.C., 2004. On the role of hydroxyl radicals in the self-cleansing capacity of the troposphere. *Atmospheric Chemistry and Physics* 4, 2337–2344.
- Murazaki, K., Hess, P., 2006. How does climate change contribute to surface ozone change over the United States? *Journal of Geophysical Research* 111, D05301. <http://dx.doi.org/10.1029/2005JD005873>.
- Nassar, R., Logan, J.A., Worden, H.M., Megretskaia, I.A., Bowman, K.W., Osterman, G.B., Thompson, A.M., Tarasick, D.W., Austin, S., Claude, H., Dubey, M.K., Hocking, W.K., Johnson, B.J., Joseph, E., Merrill, J., Morris, G.A., Newchurch, M., Oltmans, S.J., Posny, F., Schmidlin, F.J., Vomel, H., Whiteman, D.N., Witte, J.C., 2008. Validation of Tropospheric Emission Spectrometer (TES) nadir ozone profiles using ozonesonde measurements. *Journal of Geophysical Research* 113, D15S17. <http://dx.doi.org/10.1029/2007JD008819>.
- Park, R.J., Jacob, D.J., Field, B.D., Yantosca, R.M., Chin, M., 2004. Natural and trans-boundary pollution influences on sulfate–nitrate–ammonium aerosols in the United States: implications for policy. *Journal of Geophysical Research* 109, D15204. <http://dx.doi.org/10.1029/2003JD004473>.
- Rind, D., Lerner, J., Jonas, J., McLinden, C., 2007. The effects of resolution and model physics on tracer transports in the NASA Goddard Institute for Space Studies general circulation models. *Journal of Geophysical Research* 112, D09315. <http://dx.doi.org/10.1029/2006JD007476>.
- Seinfeld, J.H., Pandis, S.N., 1998. *Atmospheric Chemistry and Physics: From Air Pollution to Climate Change*, first ed. J. Wiley, New York.
- Sillman, S., Logan, J.A., Wofsy, S.C., 1990. A regional scale model for ozone in the United States with subgrid representation of urban and power plant plumes. *Journal of Geophysical Research* 95 (D5), 5731–5748. <http://dx.doi.org/10.1029/JD095iD05p05731>.
- van der Werf, G.R., Randerson, J.T., Giglio, L., Collatz, G.J., Kasibhatla, P.S., Arellano Jr., A.F., 2006. Interannual variability in global biomass burning emissions from 1997 to 2004. *Atmospheric Chemistry and Physics* 6, 3423–3441. <http://dx.doi.org/10.5194/acp-6-3423-2006>.
- van Donkelaar, A., Martin, R.V., Leaitch, W.R., Macdonald, A.M., Walker, T.W., Streets, D.G., Zhang, Q., Dunlea, E.J., Jimenez, J.L., Dibb, J.E., Huey, L.G., Weber, R., Andreae, M.O., 2008. Analysis of aircraft and satellite measurements from the Intercontinental Chemical Transport Experiment (INTEX-B) to quantify long-range transport of East Asian sulfur to Canada. *Atmospheric Chemistry and Physics* 8, 2999–3014.
- Wang, Y., Jacob, D.J., Logan, J.A., 1998. Global simulation of tropospheric O₃–NO_x–hydrocarbon chemistry: 3. Origin of tropospheric ozone and effects of non-methane hydrocarbons. *Journal of Geophysical Research* 103, 10,757–10,767. <http://dx.doi.org/10.1029/98JD00156>.
- Wang, Y., Zhang, Y., Hao, J., Luo, M., 2011. Seasonal and spatial variability of surface ozone over China: contributions from background and domestic pollution. *Atmospheric Chemistry and Physics* 11, 3511–3525. <http://dx.doi.org/10.5194/acp-11-3511-2011>.
- Wild, O., Prather, M.J., 2006. Global tropospheric ozone modeling: quantifying errors due to grid resolution. *Journal of Geophysical Research* 111, D11305. <http://dx.doi.org/10.1029/2005JD006605>.
- Wu, S., Mickley, L.J., Jacob, D.J., Logan, J.A., Yantosca, R.M., Rind, D., 2007. Why are there large differences between models in global budgets of tropospheric ozone? *Journal of Geophysical Research* 112, D05302. <http://dx.doi.org/10.1029/2006JD007801>.
- Wu, S., Mickley, L.J., Leibensperger, E.M., Jacob, D.J., Rind, D., Streets, D.G., 2008a. Effects of 2000–2050 global change on ozone air quality in the United States. *Journal of Geophysical Research* 113, D06302. <http://dx.doi.org/10.1029/2007JD008917>.
- Wu, S., Mickley, L.J., Jacob, D.J., Rind, D., Streets, D.G., 2008b. Effects of 2000–2050 changes in climate and emissions on global tropospheric ozone and the policy-relevant background surface ozone in the United States. *Journal of Geophysical Research* 113, D18312. <http://dx.doi.org/10.1029/2007JD009639>.
- Zeng, G., Pyle, J.A., 2003. Changes in tropospheric ozone between 2000 and 2100 modeled in a chemistry-climate model. *Geophysical Research Letters* 30 (7), 1392. <http://dx.doi.org/10.1029/2002GL016708>.
- Zhang, Q., Streets, D.G., Carmichael, G.R., He, K.B., Huo, H., Kannari, A., Klimont, Z., Park, I.S., Reddy, S., Fu, J.S., Chen, D., Duan, L., Lei, Y., Wang, L.T., Yao, Z.L., 2009. Asian emissions in 2006 for the NASA INTEX-B mission. *Atmospheric Chemistry and Physics* 9, 5131–5153.